

# Inorganic Electrides Formed by Alkali Metal Addition to Pure Silica Zeolites

Daryl P. Wernette, Andrew S. Ichimura,<sup>†</sup> Stephanie A. Urbin, and James L. Dye\*

Department of Chemistry, Michigan State University, East Lansing, Michigan 48824

Received September 12, 2002. Revised Manuscript Received February 5, 2003

Up to 4 Cs or Rb atoms per 32 Si atoms can be incorporated into the channels of the all-silica ( $\text{SiO}_2$ ) zeolites ITQ-4 and beta with effective oxidation states of zero. The optical properties and  $^{29}\text{Si}$  MAS NMR spectra suggest partial or complete ionization within the channels to yield  $\text{M}^+$  ions and relatively free electrons. This view is supported by a published structural model (Petkov, V.; Billinge, S. I.; Vogt, T.; Ichimura, A. S.; Dye, J. L. *Phys. Rev. Lett.* **2002**, *89*, 075502) based on pair distribution functions for Cs in ITQ-4. As with solutions of alkali metals in ammonia, however, the trapped electrons in this inorganic electride interact with the cations, and spin-pairing between adjacent electrons also occurs. The crystal morphology is unaffected by the inclusion of alkali metals. Structural distortions that reduce or eliminate long-range order are completely reversed upon oxidation and removal of the metal. At higher temperatures, Na and K can also be incorporated, but the optical spectra indicate that either substantial ionization does *not* occur or the released electrons react reversibly with the silica to form strongly reducing species.

## Introduction

Crystalline electrides in which trapped electrons serve as the counteranions to alkali cations that are encapsulated within an organic cage have been known for over 20 years.<sup>1–6</sup> The synthesis, study, and uses of organic electrides are severely hampered, however, by their thermal instability. Trapped electrons are powerful reducing agents and they destroy the organic cage at temperatures above about  $-40^\circ\text{C}$ . Even when the temperature is kept below  $-40^\circ\text{C}$ , there is still concern that partial decomposition of the sample might occur during preparation, storage, transfer, or data collection. A long-standing goal of our research has been the synthesis of thermally stable electrides.

The term “electride” has been used in a variety of contexts, including alkali metal addition to aluminosilicates,<sup>2,7</sup> in which the “excess electrons” are localized near an array of three or more alkali cations. In its original formulation, however, an electride was viewed as a “salt” in which the anions were electrons trapped in cavities or channels and separated from the cations.<sup>3,8,9</sup> Depending on the sizes of the channels that

connect the cavities, organic electrides can form Mott insulators because of electron localization,<sup>5</sup> or near metals with strong interelectron coupling.<sup>10</sup> It has even been suggested that the fully metallic compound  $\text{Li}(\text{NH}_3)_4$  may be an electride.<sup>11</sup>

Ever since Kasai and co-workers showed that electrons could be trapped in alumino-silicate zeolites by either ionizing radiation<sup>12</sup> or exposure to sodium vapor,<sup>13</sup> a large number of studies have been made on the addition products of alkali metals to such zeolites.<sup>7,13–21</sup> Such adducts exhibit a wide range of properties, from antiferromagnetism<sup>22</sup> to ferro- or ferrimagnetism,<sup>23–25</sup> various optical bands,<sup>24,26</sup> and the formation of alkali

- (8) Dye, J. L.; Yemen, M. R.; DaGue, M. G.; Lehn, J.-M. *J. Chem. Phys.* **1978**, *68*, 1665–1670.
- (9) Dye, J. L.; Ellaboudy, A. *Chem. Br.* **1984**, *20*, 210–215.
- (10) Ichimura, A. S.; Wagner, M. J.; Dye, J. L. *J. Phys. Chem. B* **2002**, *106*, 11196–11202.
- (11) Kaplan, T. A.; Harrison, J. F.; Dye, J. L.; Rencsok, R. *Phys. Rev. Lett.* **1995**, *75*, 978.
- (12) Kasai, P. H. *J. Chem. Phys.* **1965**, *43*, 3322–33277.
- (13) Rabo, J. A.; Angell, P. H.; Kasai, P. H.; Schomaker, V. *Discuss. Faraday Soc.* **1966**, *41*, 328–349.
- (14) Anderson, P. A.; Barr, D.; Edwards, P. P. *Angew. Chem., Int. Ed. Engl.* **1991**, *11*, 1501–1502.
- (15) Armstrong, A. R.; Anderson, P. A.; Woodall, L. J.; Edwards, P. P. *J. Phys. Chem.* **1994**, *98*, 9279–9284.
- (16) Bordiga, S.; Ferrero, A.; Giannello, E.; Spoto, G.; Zecchina, A. *Catal. Lett.* **1991**, *8*, 375–378.
- (17) Kelly, M. J. *J. Phys.: Condens. Matter* **1995**, *7*, 5507–5519.
- (18) Kodaira, T.; Nozue, Y.; Ohwashi, S.; Goto, T.; Terasaki, O. *Phys. Rev. B* **1993**, *48*, 12245–12252.
- (19) Nakayama, H.; Klug, D. D.; Ratcliffe, C. I.; Ripmeester, J. A. *J. Am. Chem. Soc.* **1994**, *116*, 9777–9778.
- (20) Sun, T.; Seff, K.; Heo, N. H.; Petranovskii, V. P. *Science* **1993**, *259*, 495–497.
- (21) Woodall, L. J.; Anderson, P. A.; Armstrong, A. R.; Edwards, P. P. *J. Chem. Soc., Dalton Trans.* **1996**, *719*–727.
- (22) Srdanov, V. I.; Stucky, G. D.; Lippmaa, E.; Engelhardt, G. *Phys. Rev. Lett.* **1998**, *80*, 2449–2452.
- (23) Nozue, Y.; Kodaira, T.; Ohwashi, S.; Goto, T.; Terasaki, O. *Phys. Rev. B* **1993**, *48*, 12253–12261.

\* To whom correspondence should be addressed.

† Current address: Department of Chemistry and Biochemistry, San Francisco State University, 1600 Holloway Ave., San Francisco, CA 94132.

(1) Dawes, S. B.; Ward, D. L.; Huang, R. H.; Dye, J. L. *J. Am. Chem. Soc.* **1986**, *108*, 3534–3535.

(2) Dye, J. L. *Prog. Inorg. Chem.* **1984**, *32*, 327–441.

(3) Dye, J. L. *Science* **1990**, *247*, 663–668.

(4) Dye, J. L.; Wagner, M. J.; Overney, G.; Huang, R. H.; Nagy, T. F.; Tomaneck, D. *J. Am. Chem. Soc.* **1996**, *118*, 7329–7336.

(5) Dye, J. L. *Inorg. Chem.* **1997**, *36*, 3816–3826.

(6) Xie, Q.; Huang, R. H.; Ichimura, A. S.; Phillips, R. C.; Pratt, W. P., Jr.; Dye, J. L. *J. Am. Chem. Soc.* **2000**, *122*, 6971–6978.

(7) Edwards, P. P.; Anderson, P. A.; Thomas, J. M. *Acc. Chem. Res.* **1996**, *29*, 23–29.

metal anions.<sup>19,27</sup> Alumino-silicates have pre-existing arrays of cations to which the “excess electrons” introduced by the added alkali metal are attracted. By contrast, ionization of alkali metals in all-silica zeolites would yield a cation-to-electron ratio of 1:1 as in organic electrides.

We report here the preparation and properties of thermally stable “inorganic electrides” made by adding alkali metals to the all-silica zeolites ITQ-4 (IFR)<sup>28–30</sup> and beta (BEA).<sup>31</sup> A preliminary report of this work has appeared,<sup>32</sup> and a model obtained from the differential pair distribution functions (PDFs) for cesium in ITQ-4 is described in a separate publication.<sup>33</sup> Because the powder XRD patterns for Cs in ITQ-4 showed disorder and no new peaks due to Cs, the location of the cesium species could not be directly determined. However, the PDF studies<sup>33</sup> provided detailed information about the nature of the disorder and the distribution of Cs centers within the channels of this zeolite. The overall PDF patterns for 3.6 and 4.6 Cs per unit cell in ITQ-4 showed that the *local* Si–O structure is not significantly disturbed by the incorporation of Cs, but that the *long-range* order is disrupted. The Cs differential PDF, which measures the distances of all atoms from Cs (including other Cs atoms), was best fit by a model that places Cs<sup>+</sup> ions (not Cs<sup>0</sup> or Cs<sup>-</sup>) in zigzag fashion (but without long-range order) down the 1D sinusoidal channels of ITQ-4.

On the basis of the Cs<sup>+</sup> to O distances obtained from this model, the cations are situated near the channel walls such that each Cs<sup>+</sup> can interact with a number of O atoms in the Si–O–Si structure. From the crystal structure of ITQ-4 and the PDF model, it can be shown that there are eight Cs<sup>+</sup>–O distances between 3.5 and 4.1 Å. Combining these positional results provides a picture in which the cesium atoms interact with the oxygen atoms that line the zeolite channels. This leads to ionization of the atom and delocalization of the valence electron density into the void spaces in the channels. Although the electron density is attracted to the cation through Coulombic forces, it is polarized away from the cation by the interaction of Cs<sup>+</sup> with the oxygen lone pairs.

Electron spin-pairing is ubiquitous in electrides<sup>5</sup> and in metal–ammonia solutions.<sup>34</sup> Thus, it is not surprising that magnetic susceptibilities and EPR spectra have

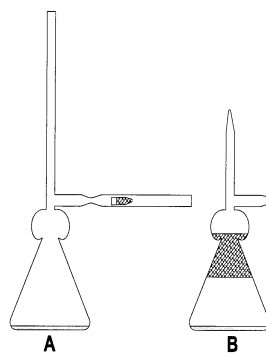


**Figure 1.** Modified Erlenmeyer flask for the addition of alkali metal to the zeolite before (A) and after (B) the metal film was made and the sidearms were sealed off.

shown that most of the electrons in the metal–zeolite systems described in this paper are also spin-paired. There is, however, a significant difference between electrides that contain organic complexants and these metal-loaded zeolites. In the former, the cations are sequestered within molecular cages or sandwiched between two complexant molecules, and the electron density has its maximum in an otherwise empty cavity. In the zeolites described in this paper, the cations and electrons coexist in the same channel, so we anticipate that the properties would depend more strongly on the alkali metal used. Indeed, it is likely that there is competition between ionization and the formation of neutral metallic species. An *ideal* inorganic electride would have separate cation and electron traps to minimize such interactions.

## Experimental Procedure

Sodium, potassium, and rubidium in glass break-seal ampules were obtained from Alfa Aesar, and cesium ampules were a gift from the Dow Chemical Company. The method used to transfer metals to small-diameter glass tubing has been previously described.<sup>35</sup> All chemicals needed for the preparation of structure-directing agents (SDAs) and for the synthesis of the zeolites were obtained from Sigma-Aldrich.

Two pure silica zeolites with low defect concentrations, ITQ-4<sup>28–30</sup> and beta,<sup>31</sup> were synthesized and calcined by previously reported methods that use fluoride as a mineralizer. After synthesis, scanning electron microscope images, powder X-ray diffraction patterns, and solid state <sup>29</sup>Si MAS NMR methods were used to verify the identity of the zeolites as well as the low defect concentrations. The calcined zeolite was evacuated with intermittent heating to remove any volatiles from the pores and was then stored in a helium-filled glovebox.

The samples were loaded with alkali metals in the glovebox by adding a known amount of zeolite to a preparatory flask (Figure 1) with an appropriate mass of alkali metal placed into a sidearm of the flask. The alkali metal (contained in an open-ended glass ampule) was inserted into the sidearm of the flask and the zeolite was added via a funnel to the bottom of the flask. The open tubes were capped with UltraTorr fittings, a closed tube, and a Kontes 4-mm Teflon stopcock. After removal from the glovebox and evacuation, the sidearm was flame-sealed behind the metal ampule, the metal was distilled into the body of the flask, and the flask was sealed off at a pressure of 10<sup>-5</sup> Torr or less. The collection bulb, just below the sidearm, was used to prevent liquid metal from running down the flask onto the zeolite. Although cesium could be introduced at room temperature over a period of several days, it was usually necessary to heat the entire closed system to increase the vapor pressure of the metal to 10<sup>-5</sup> Torr or higher. The flask was

- (24) Kodaira, T.; Nozue, Y.; Ohwashi, S.; Goto, T.; Terasaki, O. *Phys. Rev. B* **1993**, *48*, 12245–12252.
- (25) Ikeda, T.; Kodaira, T.; Izumi, F.; Kamiyama, T.; Oshima, K. *Chem. Phys. Lett.* **2000**, *318*, 93–101.
- (26) Blake, N. P.; Srdanov, V. I.; Stucky, G. D.; Metiu, H. *J. Chem. Phys.* **1996**, *104*, 8271–8279.
- (27) Terskikh, V. V.; Moudrakovski, I. L.; Ratcliffe, C. I.; Ripmeester, J. A.; Reinhold, C. J.; Anderson, P. A.; Edwards, P. P. *J. Am. Chem. Soc.* **2001**, *123*, 2891–2892.
- (28) Camblor, M. A.; Corma, A.; Villaescusa, L. A. *Chem. Commun.* **1997**, *1997*, 749–750.
- (29) Barrett, P. A.; Camblor, M. A.; Corma, A.; Jones, R. H.; Villaescusa, L. A. *Chem. Mater.* **1997**, *9*, 1713–1715.
- (30) Barrett, P. A.; Camblor, M. A.; Corma, A.; Jones, R. H.; Villaescusa, L. A. *J. Phys. Chem. B* **1998**, *102*, 4147–4155.
- (31) Camblor, M. A.; Corma, A.; Valencia, S. *Chem. Commun.* **1996**, *1996*, 2365–2366.
- (32) Ichimura, A. S.; Dye, J. L.; Camblor, M. A.; Villaescusa, L. A. *J. Am. Chem. Soc.* **2002**, *124*, 1170–1171.
- (33) Petkov, V.; Billinge, S. I.; Vogt, T.; Ichimura, A. S.; Dye, J. L. *Phys. Rev. Lett.* **2002**, *89*, 75502.
- (34) Thompson, J. C. *Electrons in Liquid Ammonia*; Oxford University Press: Oxford, 1976.

rotated and bumped mechanically while being heated to continuously expose new surface area to the vapor. Occasional brief exposure to an ultrasonic bath was also used; however, excess ultrasonication was found to shatter these zeolite crystals.

The overall amount of unoxidized metal per unit cell (u.c.) of the zeolite ( $\text{Si}_{32}\text{O}_{64}$  for ITQ-4 and  $\text{Si}_{64}\text{O}_{128}$  for beta) was determined by measuring the amount of hydrogen gas produced by the reduction of water. For comparison purposes we define the *reducing power* as twice the number of molecules of  $\text{H}_2$  collected per 32 Si atoms. The hydrogen was collected with a modified mercury-filled Toepler pump.<sup>36,37</sup> The metal hydroxide formed within the zeolite was then neutralized with excess 0.01 M HCl and back-titrated with NaOH. A JEOL 6400V scanning electron microscope (SEM) with energy-dispersive analysis capabilities (EDA) was used to image the crystallite morphology and to provide an approximate check of both the overall alkali metal concentration and its uniformity across the sample. A Rigaku RU-200B X-ray diffractometer was used to obtain powder X-ray diffraction (XRD) patterns (in 0.7-mm-diameter capillaries) of three types of samples: metal-loaded, air-oxidized, and neutralized-washed.

Diffuse optical reflectance spectra were obtained by using a Harrick collection orb with quartz lenses inside a helium-filled glovebox. Fiber-optic cables connected the collection system to an external Guided Wave (GW) Model 260 spectrometer. The UV-vis range of the spectrum (230–600 nm) was collected by using a GW DTL 200 deuterium source, Ocean Optics p600-2 UV-vis fiber-optic cables, 1200 line/mm grating and a PMT detector module. The VIS-IR region was collected with the GW internal tungsten source, GW 04-2B vis-IR fiber-optic cables, 300 line/mm grating, and silicon (400–1135 nm) and lead sulfide (1136–2000 nm) detector modules. The spectra were collected as reflectance and converted to approximate absorbance units with the Kubelka-Munk (KM) function.<sup>24,38</sup>

A Varian VXR 400S NMR spectrometer was used to collect  $^{29}\text{Si}$  MAS NMR spectra for every synthesized zeolite sample. Solid-state  $^{29}\text{Si}$  and  $^{133}\text{Cs}$  MAS NMR spectra were acquired for a number of samples that contained the metal, followed, in some cases, by air oxidation and collection of NMR spectra for both nuclei. The thermal properties of the zeolites and metal-loaded samples, sealed in aluminum pans, were determined with a Shimadzu DSC-50 differential scanning calorimeter (DSC).

## Results

**General Observations.** As alkali metal vapor makes contact with the zeolite during loading, the pure white surface changes color to gray or blue. Continuous agitation was necessary to expose new surfaces. The colors ranged from gray-brown for sodium, to light blue-gray for potassium, to bright blue for rubidium, and to darker gray-blue for cesium. The rate of this color change depends on the vapor pressure of the metal being added and the dimensionality of the zeolite channels. Zeolite ITQ-4, with “one-dimensional” channels, required longer incorporation times or higher temperatures than zeolite beta, which has three-dimensional channels that allow more migration routes. Cesium, at vapor pressures between  $10^{-5}$  and  $10^{-4}$  Torr, can be introduced into zeolite beta overnight and into ITQ-4 over a period of several days. The other three metal preparations required higher temperatures to reach the same vapor pressure. Typical preparation temperatures for Cs, Rb, K, and Na were 50, 70, 125, and 180 °C,

respectively. With the increased temperature needed to incorporate potassium, and especially sodium, the blue-gray color changed to a tan or brown color. This color change also occurs for rubidium and cesium samples when they are heated to temperatures above 90 °C. SEM images of metals in ITQ-4 or beta showed no change in crystal morphology upon loading and subsequent oxidation, up to metal concentrations of 4.0 atoms per 32 Si. DSC measurements up to 400 °C on freshly prepared samples showed no heat absorption or emission. This indicates the absence of exothermic reactions of the alkali metal with the zeolite, at least on the hour time scale.

**Analyses.** Disappearance of the metal film during synthesis indicated complete absorption of the alkali metal into the zeolite. Three important considerations need to be addressed, however. These are (1) the total metal concentration, (2) the oxidation state of the metal within the zeolite, and (3) the uniformity of the metal distribution among the crystallites and within each crystallite.

We cannot be certain that a reduction product of the  $\text{SiO}_2$  zeolite would be unable to reduce water to form hydrogen. If it does so, however, even for Na- and K-loaded samples, the zeolite structure is fully restored upon reaction with water, as indicated by the retention of morphology, XRD pattern, and (studied only with Cs-loaded samples) the  $^{29}\text{Si}$  NMR spectrum. Thus, the quantitative formation of  $\text{H}_2$  demonstrates the presence of an *effective* zero oxidation state for the metal. Furthermore, the reduction potential of included cesium was shown to be similar to that of the metal because even benzene could be reduced to the radical anion within the pores of the zeolite. The total *unoxidized* metal concentration initially present was determined from the amount of  $\text{H}_2$  formed by reaction with water. The acid-base titration of the product yielded the *total* metal concentration in both the 0 and the +1 oxidation states. Although strong bases can dissolve silica, the process is slow enough that rapid neutralization restored the zeolite properties. Indeed, such recovered samples could be reused if desired.

Every sample was analyzed by weighing out about 20 mg each time. As shown in Figure 2A, freshly prepared samples generally gave the same results for both  $\text{H}_2$  collection and pH titration. This indicates that the concentration of reducible defects is so small that it cannot be determined by this analysis method. An additional *approximate* determination of the total concentration of alkali metal in both the 0 and +1 oxidation states, and the uniformity of this concentration, was obtained by SEM-EDA analysis. Figure 2B shows that the concentrations determined by EDA are systematically higher than those from hydrogen collection and titration, probably because of higher surface concentrations. The SEM images of the pure zeolites and of air-oxidized metal-containing samples were the same as those in the literature.<sup>30,39</sup> Crystallite sizes ranged from 1 to 10  $\mu\text{m}$ . At loadings above 4.0 metal atoms per 32 Si for K and Cs in ITQ-4, the SEM images showed some crystallite degradation (not studied for samples with Na or Rb).

(36) Dewald, R. R.; Dye, J. L. *J. Phys. Chem.* **1964**, *68*, 128–134.

(37) VanEck, B.; Le, L. D.; Issa, D.; Dye, J. L. *Inorg. Chem.* **1982**, *21*, 1966–1970.

(38) Kubelka, P.; Munk, F. *Z. Tech. Phys.* **1931**, *12*, 593–601.

(39) Camblor, M. A.; Corma, A.; Valencia, S. *J. Mater. Chem.* **1998**, *8*, 2137–2145.

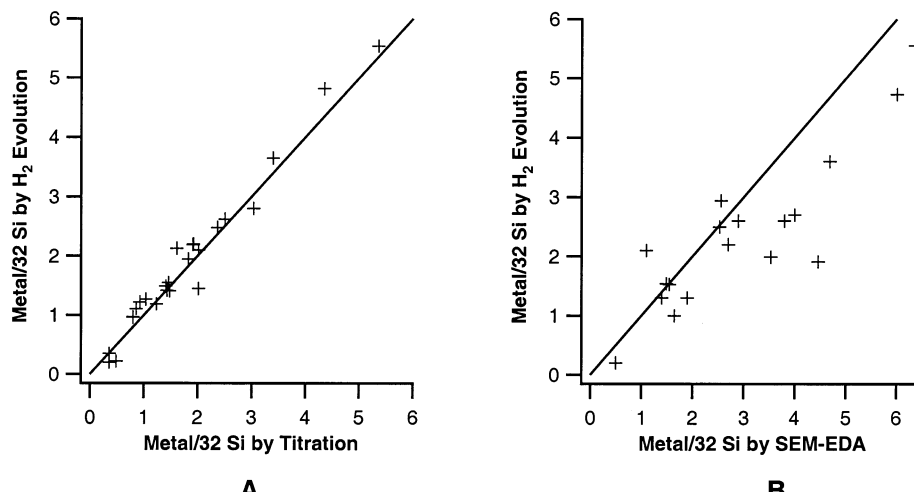


**Figure 2.** Alkali metal concentrations per 32 Si (reducing power) for various loaded samples plotted against the concentrations determined by titration (A) and SEM-EDA (B). The solid lines represent perfect agreement.

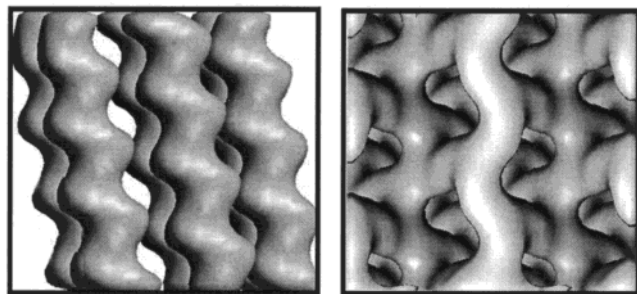


**Figure 3.** Views of the channel geometry in ITQ-4 (left) and in polytype B of zeolite beta (right).

**Structural Considerations.** The ITQ-4 and beta zeolites used in this study and in previous work<sup>32</sup> are all-silica zeolites that have low concentrations of defects. The absence of a broad peak at about  $-100$  ppm in the  $^{29}\text{Si}$  MAS NMR spectra, which is characteristic of Si–O<sup>–</sup> defects, shows that there are not more than  $\sim 0.4$  defects of this type per 32 Si. The initial study used ITQ-4<sup>28–30</sup> with its system of 1D channels and ITQ-7<sup>40</sup> with a 3D array of intersecting channels. The precursors to the SDA for the synthesis of ITQ-7 are no longer available, so zeolite beta, which also has a 3D collection of intersecting channels,<sup>31,41</sup> was used instead. Figure 3 shows the geometry of the channels in ITQ-4 and in polytype B of zeolite beta. A hard-sphere model with fixed van der Waals radii<sup>42</sup> yields minimum channel diameters of 6.4 and 6.0 Å, respectively. These are large enough to permit easy migration of alkali metal atoms into and through the zeolite. The available space in ITQ-4 is adequate for the incorporation of up to four alkali metal atoms per unit cell (of 32 Si) without undue crowding. In zeolite beta there are eight channel intersections per unit cell (of 64 Si), so that comparable loadings of 4 metal atoms per 32 Si can be readily accommodated in both zeolites.

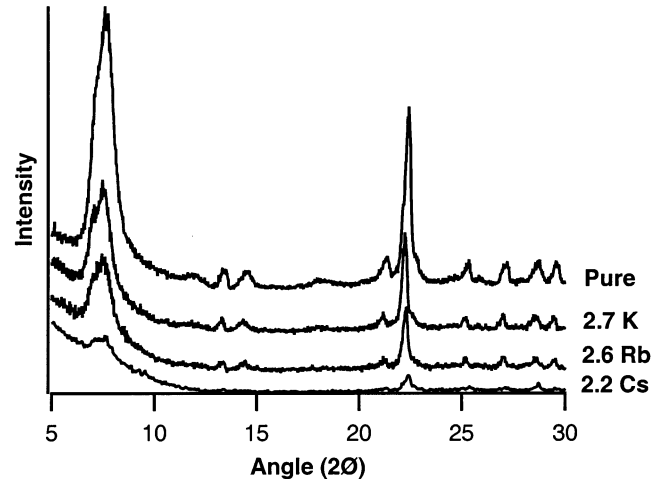


**Figure 4.** X-ray powder diffraction patterns for zeolite beta, pure and loaded with various alkali metals. The number of metal atoms per 32 Si is given on the right. The patterns have been vertically shifted for clarity but maintain their respective intensities.

The XRD patterns shown in Figure 4 for three alkali metals in zeolite beta have only the features that are also present in the pure zeolite. This was also shown previously for various loadings of Cs in ITQ-4.<sup>32</sup> Clearly, the alkali metals are not completely ordered within the zeolite framework. In addition, the XRD pattern shows increasing disorder of the silica lattice with both increased loading and as the metal is changed from K to Rb to Cs. The decreased XRD intensity is not simply due to increased X-ray absorption by the added metal. Even at the heaviest loading with Cs, the overall electron density increases by only 28% whereas there is a 30-fold decrease in the XRD peak intensity. The PDF results<sup>33</sup> also clearly showed a loss in long-range order from that of the pure zeolite. The remarkable feature of this structural distortion is that it is fully reversible. Although air oxidation of heavily loaded samples gives the same XRD pattern as that before oxidation, the neutralization and washing of the samples for all metals completely restores it.

**Optical Spectra.** Diffuse optical reflectance spectra were collected for the loaded zeolite samples and converted to apparent absorbance with the Kubelka–

(40) Villaescusa, L. A.; Barrett, P. A.; Cambor, M. A. *Angew. Chem., Int. Ed.* **1999**, *38*, 1997–2000.

(41) Higgins, J. B.; LaPierre, R. B.; Schlenker, J. L.; Rohrman, A. C.; Wood, J. D.; Kerr, G. T.; Rohrbaugh, W. J. *Zeolites* **1988**, *8*, 446–452.

(42) Nagy, T. F.; Mahanti, S. D.; Dye, J. L. *Zeolites* **1997**, *19*, 57–64.

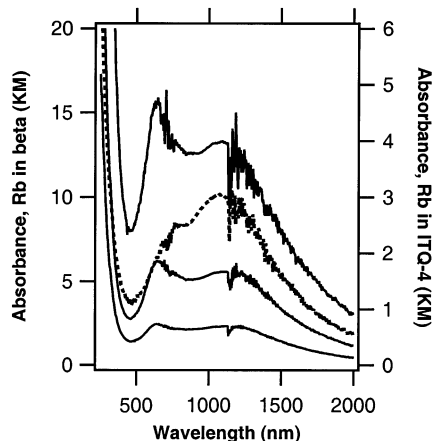


**Figure 5.** Optical spectra for various loadings of Rb in zeolite beta. From top to bottom (solid lines) the metal loadings per 32 Si atoms are 3.3, 2.7, and 1.6. Also included is a spectrum of 1.0 Rb/32 Si in ITQ-4 (dashed line and right axis). A corresponding graph for Cs in ITQ-4 is given elsewhere.<sup>32</sup>

Munk function.<sup>24,38</sup> All samples with Rb and Cs show a broad near-IR absorbance with a maximum at 1200–1500 nm that is strikingly similar to those of solvated electrons in ammonia and amines<sup>34</sup> as well as those of crystalline electrides.<sup>43</sup> The spectra shown in Figure 5 for Rb in beta are similar to those of Rb (dashed line in Figure 5) in ITQ-4. As shown in Figure 2 of the previous paper,<sup>32</sup> low Cs concentrations in ITQ-4 have only the IR peak. For Rb and Cs in beta and for higher metal concentrations of Cs in ITQ-4, a visible peak or shoulder occurs at 600–800 nm as well as a continuous increase in absorbance on the blue end of the spectrum.

There is no peak at short wavelengths down to the limit of our optical system (240 nm). Only a rising absorbance is observed for Rb and Cs. This absorbance edge could reflect a shift in the silica absorbance toward the visible, as occurs when alkali oxides are incorporated into pure silica.<sup>44</sup> However, this UV rise disappears when the sample is exposed to air for 10 min, even though the alkali cations are still present. When the spectra displayed in Figure 5 for Rb in zeolite beta are normalized at the wavelength of the IR peak, the UV absorbances coincide. This shows that the onset of the rise is nearly independent of concentration.

The spectra of Na and K in zeolite beta are strikingly different from those of Rb and Cs. Representative spectral shapes are shown in Figure 6. For Na and K there is no IR peak, even at light loadings, although for K there is a “tail” that extends into the IR region. The UV-vis region shows a rising absorbance at short wavelengths, as occurs with Rb and Cs. However, there are also shoulders present on the UV rising absorbance that indicate the presence of unresolved peaks. Attempts to deconvolute the spectra in this region by subtracting the shape of the rising absorbance of Cs suggested the presence of underlying absorbance peaks at about 330 and 360 nm for Na and K, respectively.

For all metals the absorbance generally increased with increasing metal concentration. However, although spectral shapes are reliable, caution must be used in

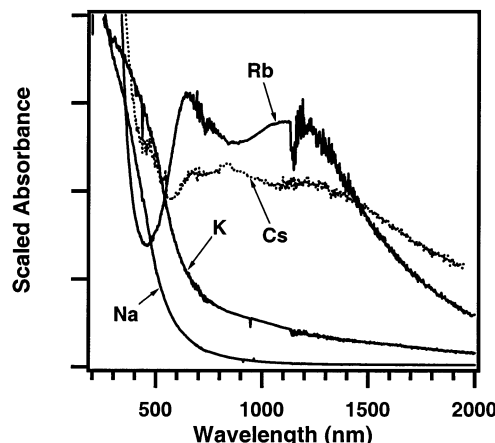


**Figure 6.** Representative spectral shapes of zeolite beta loaded with various alkali metals. The amplitudes have been arbitrarily scaled for clarity.

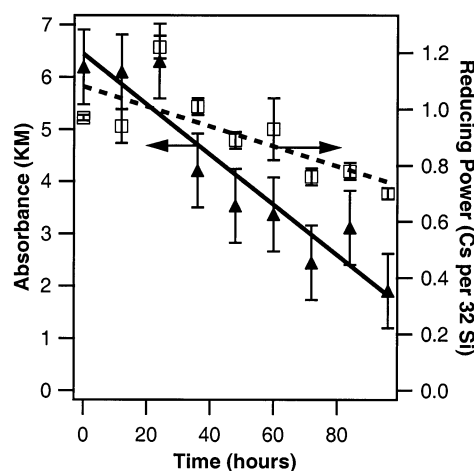


**Figure 7.** Variations with time upon exposure to the glovebox atmosphere (<0.3 ppm oxygen) of the reducing power (squares and dashed line) and the absorbance (triangles and solid line).

drawing conclusions from the intensity. Flatness of the powder surface is important as well as particle size. Despite all attempts to ensure uniformity of the procedures, repeated measurements of the KM absorbance of different samples from the same source yielded standard deviations of  $\pm 20\%$  of the peak absorbance.

As expected, oxidation, which occurred slowly even in the helium-filled glovebox, caused bleaching of the absorbance and a lower reducing power. A control sample that was kept *under vacuum* at the ambient box temperature was essentially unchanged in both its spectrum and analysis during the time that a portion of the same sample that was exposed to the box atmosphere had almost totally bleached. These experiments demonstrate that cesium-loaded ITQ-4 is very reactive, even toward trace amounts of oxygen.

To determine the rate of oxygen absorption in the glovebox and its effect on the optical absorbance and reducing power, a sample of Cs in ITQ-4 at a concentration of 1.24 Cs/32 Si was divided into 9 portions and studied over a time span of 96 h without disturbing the glovebox atmosphere. Initially, and after each 12-h period, the reflectance spectrum was obtained of a sample that had been standing since the start of the experiment in an open vial (occasionally shaken to provide mixing). At the time the spectrum was obtained,

(43) Huang, R. H.; Faber, M. K.; Moeggenborg, K. J.; Ward, D. L.; Dye, J. L. *Nature* **1988**, 331, 599–601.

(44) Sigel, C. H., Jr. *J. Phys. Chem. Solids* **1971**, 32, 2373–2383.

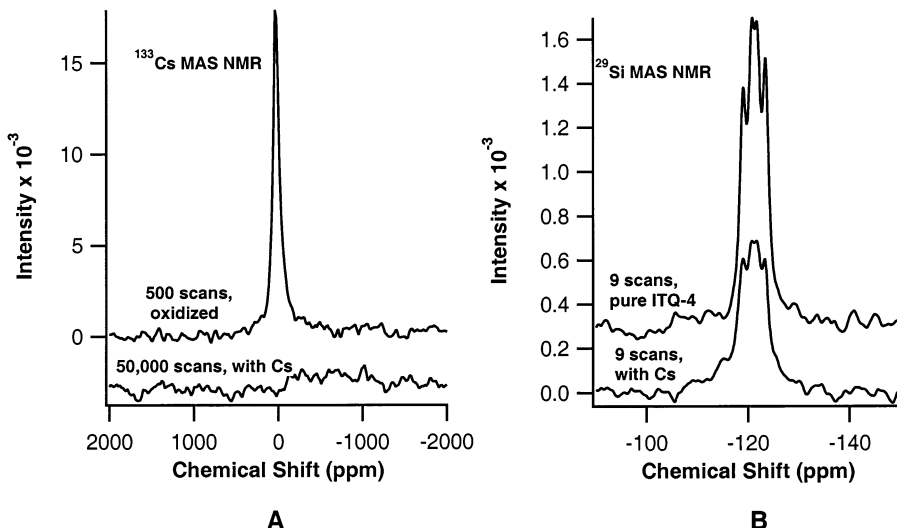


**Figure 8.** Solid-state MAS NMR spectra of  $^{133}\text{Cs}$  (A) and  $^{29}\text{Si}$  (B) at loadings of 1.1 (A) and 2.7 (B) Cs/u.c. in ITQ-4. The spectra in (A) were obtained with pulse delay times of 1 s while those in (B) used pulse delay times of 1.5 h. The spectra have been displaced vertically for clarity.

a portion of the same sample was put into an analysis flask, evacuated, and sealed without removal from the glovebox. After completion of the set of experiments, all analysis flasks were removed from the glovebox and the contents were analyzed by hydrogen evolution and pH titration. Over the 96-h time span, oxidation caused the bulk reducing power to decline steadily by a total of about 40%. However, as shown in Figure 7, even though stirred samples were examined, the absorbance decreased by a total of about 70%.

The decrease in absorbance without a concomitant decrease in reducing power must arise from the limited depth probed by reflectance measurements. Even in the absence of an absorber, inter- and intracrystallite light scattering must limit the effective depth. At the low oxygen levels in the glovebox ( $<0.3$  ppm) oxidation occurs slowly, so restricted migration through the channels would cause the surface regions to bleach first.

**Solid-State NMR Spectra.** No detectable signal was found in the  $^{133}\text{Cs}$  MAS NMR spectra of Cs-loaded samples, even when long pulse delay times were used, but as shown in Figure 8A, air oxidation yielded a peak at the characteristic chemical shift of  $\text{Cs}^+$  with a pulse delay time of 1.0 s. The  $^{29}\text{Si}$  MAS NMR spectra of the pure degassed zeolites matched those in the literature<sup>30,31</sup> and, with a pulse delay time of 90 s, could be easily detected with fewer than 10 scans. However, upon addition of alkali metal to either of the zeolites, little or no signal could be detected at pulse delay times up to 600 s, even with a large number of scans. It was originally thought<sup>32</sup> that this was caused by dipolar coupling of delocalized electrons to all of the silicon nuclei, but the behavior persisted, even at concentrations as low as 0.3 Cs/u.c. At such concentrations, Coulomb attraction between the cation and the electron would prevent such long-range interactions. By systematic variation of the pulse delay time, full  $T_1$  relaxation was found to require more than 1 h! Evidently, the metal removes traces of a relaxation agent (such as oxygen).

With pulse delay times of 1.5 h it was possible to compare the  $^{29}\text{Si}$  MAS NMR spectra of Cs-loaded samples with those of pure ITQ-4. Figure 8B shows that

the signal intensity of a sample with 2.7 Cs/u.c. is about half that of the pure zeolite. The decrease in signal amplitude as well as that of the total integrated intensity was measured. For samples with 1.0, 2.7, and 3.3 Cs/u.c., the integrated intensities were respectively 51, 63, and 61% of those of pure ITQ-4. Measurements of the spectra of pure degassed ITQ-4 were made both before and after the runs at 1.0 and 3.3 Cs/u.c. to be sure that the reduction in signal was not caused by instrumental drift during such long time periods. These experiments show that nearly half of the Si nuclei are NMR silent, even at loadings with only one cesium per unit cell. This presumably occurs because of substantial line broadening caused by dipolar interaction between the electron and nuclear spins.

## Conclusions

The all-silica zeolites ITQ-4, ITQ-7, and beta can absorb up to 4.0 alkali metal atoms per 32 Si atoms without permanent structural changes. The color change of heated samples from blue-gray to tan or brown prompted concern that the alkali metals may reduce the silica lattice irreversibly at high temperatures. There are, however, compelling indications that such an "annealing" reaction, if it occurs at all, is fully reversible upon removal of the metal. The reducing power of all samples remained essentially unchanged, even after heating at temperatures up to 300 °C. After thorough washing of neutralized samples, the XRD pattern and  $^{29}\text{Si}$  MAS NMR spectrum was indistinguishable from that of the pure silica zeolite. Despite these indications that reaction with silica does not cause extensive changes, the nature of samples that have been heated above 100 °C, especially for samples with Na or K, may be different from those of Cs and Rb since reversible reduction of the zeolite cannot be ruled out. The behavior of samples with Rb or Cs, prepared at lower temperatures, is more indicative of metal incorporation in the channels with little or no reduction of the silica framework.

In contrast to the addition of alkali metals to alumino-silica zeolites, which have pre-existing groups of alkali

cations to which the "extra" electrons can be attracted, in the present case there is only one ionizable electron per metal center, as in organic electrides. The prominent broad absorption band in the near-IR region of the optical spectrum of Cs- and Rb-doped samples strongly suggests at least partial ionization to form  $M^+$  and nearly-free electrons. This view is supported by the Cs PDF results,<sup>33</sup> which indicate the presence of zigzag chains of  $Cs^+$  ions, even at loadings as high as 4 Cs/u.c. Since the cation is not sequestered within a separate cage, but rather shares the zeolite channel with the ionized electron,  $Cs^+$  and  $e^-$  are free to interact with each other. This may be similar to the formation of contact ion pairs in solution. One model for the formation of cation–electron pairs in metal–amine solutions proposes a continuum between solvent-shared ion pairs in which both the cation and the electron remain solvated and "expanded atoms" in which the extent of solvation of the pair decreases as the ion–solvent interaction energy decreases.<sup>45</sup> In the present case, the competition is between the energy of interaction of  $M^+$  with the oxygens of silica and the Coulomb attraction between  $M^+$  and  $e^-$ . According to this picture, the near-IR peak is attributed to nearly free electrons, but these are also attracted to the cations and may be similar to atomic Rydberg states. The concentration dependence of the absorbance of Rb in zeolite beta shown in Figure 5 and that of Cs in ITQ-4 shown in a previous paper<sup>32</sup> suggests that the visible peak may result from electron attraction to pairs or chains of adjacent alkali metal cations within the zeolite channels. Alternatively, it may be the result of the decrease in free space available to the electron.

The rising absorbance at the UV end of the spectra is present for all metals in both zeolites. Since it disappears upon oxidation, the effect is not simply caused by the presence of alkali cations. Instead, incorporation of metal either introduces new energy bands below the level of the empty excited state bands of the pure zeolite or it lowers the energy of the normally unoccupied excited  $SiO_2$  bands. The UV absorption would then result from excitation of electrons from the valence band of  $SiO_2$  to the newly introduced or modified bands. Another similarity between these metal–zeolite systems and metal–ammonia solutions is the diamagnetic nature of even the more dilute samples. Spin-pairing, as in metal–ammonia solutions of comparable concentration ( $\sim 1$  M), is extensive in these systems.

The *apparent* absence of a  $^{29}Si$  MAS NMR signal in these metal-containing zeolites was originally thought<sup>32</sup> to result from extensive delocalization of the electron and resultant dipolar or contact broadening of the NMR signal. However, the present results show that the failure to detect the  $^{29}Si$  MAS NMR signal at intermediate concentrations in the initial studies was the result of the extremely long spin-lattice relaxation times. In the present study, with pulse delay times of 1.5 h, signals from  $^{29}Si$  were detected at all loadings. They were, however, significantly reduced in both peak amplitude and integrated intensity, even at loadings of only 1.0 Cs/u.c. Presumably, silicon nuclei adjacent to the channels interact strongly with the electrons, and

the effect is equally pronounced at both 1.0 and 3.3 Cs/u.c. This provides additional evidence for ionization of Cs and electron delocalization in the channels. The extent of electron spin-pairing probably also plays a role since the broadening effect of spin-paired electrons on the  $^{29}Si$  MAS NMR spectrum would be smaller than that of unpaired electron spins.

As indicated above, the structural, optical, and magnetic properties of Cs in zeolite ITQ-4 all support the designation of this material as an "inorganic electride". Most of the early experiments concentrated on the addition of cesium to all-silica zeolites because Cs could be introduced at lower temperatures and offered an easily detectable nucleus for NMR studies. The extensive studies with Cs and Rb in ITQ-4 and zeolite beta described in the present paper show that Rb behaves in a fashion similar to Cs. The only significant difference is the retention of a visible absorption peak for Rb-loaded samples even at low concentrations. The model that best describes the behavior of Cs and Rb in both ITQ-4 and zeolite beta presumes ionization to yield a zigzag chain of cations in the channels, with nearly free electrons in the intermediate spaces. The persistence of spin-pairing at lower doping levels suggests that loose dimers or chains of ions and electrons are favored over separate  $Cs^+e^-$  species.

Potassium and sodium could be added to both ITQ-4 and beta at higher temperatures to provide up to 4 metal atoms per  $^{32}Si$  without *irreversible* changes in the structure. The retention of the reducing power showed that, as with Rb and Cs, these adducts could reduce water to produce hydrogen quantitatively. In contrast to Rb and Cs, however, the optical spectra did *not* show an appreciable near-IR peak. The absence of this peak of the "solvated electron" shows that ionization of K and Na to form the cations and trapped electrons either does not occur to a significant extent, or is followed by reaction of the electrons with the silica as a result of heating. It is possible that K and Na remain as neutral atoms or chains of atoms, with only slight polarization of the charge. However, the well-known optical peaks of alkali metal atoms or dimers are *not* present. Another possibility, which could also occur for Rb and Cs at higher temperatures, is slow, reversible formation of silicon-based radicals or anions. This would involve expanding the coordination sphere of silicon from four to five. Such expansion has been noted for these zeolites with  $F^-$  as a fifth ligand coordinated to Si along with four oxygens.<sup>30</sup> There is, however, currently no direct evidence for formation of such species in metal-loaded zeolites. The retention of the structure and crystallite morphology indicates that the rupture of Si–O bonds is unlikely. If reduction of the host zeolite by K or Na occurs, it must be simple addition of an electron to produce a highly reducing center that can revert to the original  $SiO_2$  structure upon oxidation. Additional studies on these adducts are in progress as well as more comprehensive studies of the magnetic properties of all adducts.

**Acknowledgment.** This work was supported in part by the U.S. National Science Foundation under Grant DMR 9988881 and by the Michigan State University

Center for Fundamental Materials Research. We are grateful to the Camille and Henry Dreyfus Foundation for the support of D.P.W. and S.A.U. by a Senior Scientist Mentor Award to J.L.D. We thank M. Camblor and M. Villaescusa for initial samples of ITQ-4 and for much helpful information about these zeolites, R. Huang

for help with analyses, V. Petkov and S. Billinge for measurement and interpretation of the PDF results, and M. Vlassa and J. Jackson for synthesis of the SDAs used for zeolite synthesis.

CM020906Z